The Deep-Space Optical Channel: I. Noise Mechanisms

J. Katz
Communications Systems Research Section

The noise due to various sources in the deep space optical channel with a space-based receiver is analyzed. It is found that the worst case conditions occur during the encounter phase with planets.

I. Introduction

The DSN is currently considering optical frequencies for deep space communications. The basic parameters of optical communication systems are reviewed in Ref. 1. It is clear that a comprehensive understanding of the various noise mechanisms existing in the channel must supplement any system design.

It is the purpose of this article to discuss the effects of the noise in the optical link. In the following it is assumed that the receiving station of the link is located in space. This seems almost a necessity if one wants to utilize the potential advantages of optical communication. When the receiving telescope is located on earth, additional disturbing effects must be taken into account. Those are not considered here, and can be found elsewhere (Ref. 2).

II. Noise in the Optical Link

In this part we analyze the noise mechanisms that exist in the deep space optical link. First we consider the noise that exists in the channel, i.e., background photons in the propagating medium. Then the various noise components in the receiver are reviewed.

Assuming that the receiving telescope is located in space, the three main sources of noise in the optical region (from UV to IR) of the spectrum are:

(1) Zodiacal light (ZL).

(2) Integrated star light (ISL) from our galaxy (the "Milky Way").

(3) Noise from planets in flyby encounters.

The first two sources are spacially continuous. The third source, and noise from other similar sources (i.e., bright stars), is discrete. Less important noise sources are from diffuse galactic and extragalactic contributions. At certain wavelengths the background radiation can be very much higher due to the existence of specific atomic transitions. However, the number of such strong lines is very small and all of them lie in the UV region.

If the receiver is located on the earth, then, in addition to atmospheric attenuation, there will be noise due to airglow, scattered sunlight, moonlight, and other scattering phenomena in the atmosphere. These effects will not be discussed here.

A. Zodiacal Light (Refs. 3, 4, 5, 8, and 9)

Zodiacal light is sunlight reflected by interplanetary dust. It has both spectral and spatial features. In its spectral dependence, we distinguish between two regions. For wavelengths shorter than about 3 μm, the spectrum is similar to that of the sun, i.e., a black body at approximately 5700 K. For wavelengths longer than 3 μm, the spectrum is mainly due to self-thermal radiation of the dust (i.e., similar to a 500 K black body). The spatial features of the zodiacal light are due to its distribution in the solar system (a disk in the ecliptic plane, about 4 AU in diameter and about 0.5 AU in height) and due to the angular dependence of the light scattering mechanism.

Table 2 of Ref. 3 contains information about the amount of zodiacal light for different directions of observation. The data in that table is for $\lambda = 5500$ Å, and the results should be divided by a factor of two when applied to our case (i.e., $\lambda \sim 0.8$ to 0.9 m). Figure 1 presents the results for the most common case, which is operation in or about the ecliptic plane. As an example, for $\epsilon = 90$ deg, which is a typical case (the meaning of ϵ is explained in the insert of Fig. 1), we obtain $n_\lambda \sim 7 \times 10^8$ ph $\cdot$ s^{-1} $\cdot$ cm^{-2} $\cdot$ m^{-1} $\cdot$ sr^{-1}. For a possible system design (which assumes the Large Space Telescope (LST), as the receiving antenna, a 2-μrad detector field of view and a 10 Å optical filter in front of the detector), this translates to about 10^{-2} noise photons per second.

B. Integrated Starlight (Refs. 3, 6, 7, 8, and 9)

Integrated starlight comes from direct starlight and from starlight scattered by interstellar dust. As zodiacal light, integrated starlight also has spectral and spatial features. For wavelengths shorter than 0.4 μm, the spectrum contains some yet unexplained details, with an apparent minimum wavelength in the 0.2 to 0.3 μm region ($n_\lambda \sim 10^8$ ph $\cdot$ s^{-1} $\cdot$ cm^{-2} $\cdot$ μm^{-1} $\cdot$ sr^{-1}). For wavelengths longer than 0.4 μm, the spectrum is similar to that of a star that is somewhat hotter than the sun. The amount of noise is maximum in the galactic plane, and is about one order of magnitude lower at high galactic latitudes. A typical maximum value near the galactic plane is about $n_\lambda \sim 10^9$ ph $\cdot$ s^{-1} $\cdot$ cm^{-2} $\cdot$ μm^{-1} $\cdot$ sr^{-1} at 0.9 μm. This is about the same as that for zodiacal light.

C. Noise from Planets in Flyby Situations

When a spacecraft carrying an optical transmitter is in the encounter phase with a planet, the main source of received background noise is sunlight reflected from the planet. The irradiance E_λ at the receiving aperture plane is given by (Ref. 10):

$$E_\lambda = \frac{P_\lambda H_\lambda}{R_{P_\odot}^2 \left(\frac{R}{R_p}\right)^2}, \quad \frac{\text{ph}}{\text{sec} \cdot \text{cm}^2 \cdot \mu\text{m}} \tag{1}$$

where

$H_\lambda = 4.5 \cdot 10^{17} \frac{\text{ph}}{\text{sec} \cdot \text{cm}^2 \cdot \mu\text{m}}$ at 0.9 μm (sun irradiance at 1 AU)

P_λ = geometric albedo of the planet (related to the reflection coefficient)

$R_{P_\odot}$ = sun-planet distance, AU

R = Earth-planet distance, km

R_p = Planet radius, km

Relevant data for such calculations appear in Table 1. (We assume $R = R_{P_\odot}$.) The last column of Table 1 presents the results for the amount of noise photons per second that are received in the system described earlier in this section. The detailed dependence of the amount of noise photons collected on the receiving telescope field of view is shown in Fig. 2, which also includes, for comparison, the noise due to the following sources:

(1) Noise from the sky; we have this noise when the receiver is located on earth (daytime and nighttime conditions).

(2) Noise from the zodiacal light and from the integrated starlight (considered in the previous sections).

(3) Noise from a weak star ($m_v = 6$) in the field of view.

We can conclude this section by saying that when the receiver is located in space, the dominant noise mechanism is the background noise of the planets during flyby encounters. However, this noise is still much lower than that for daytime reception with earth-based telescopes.

III. Noise in the Optical Receiver

In this section we will calculate the total amount of noise in the receiver. Again, we will assume that the optical receiver is composed of the large space telescope (Ref. 11) followed by a quantum detector. The telescope aperture is 2.4 m and the detector field of view is assumed to be 2 μrad.

A block diagram depicting the major noise components in the receiver is shown in Fig. 3. We will follow this figure in calculating the magnitude of the noise components.

a. N_b is the background radiation. Taking a Jupiter flyby as an example, we have (see Table 1) about $2 \cdot 10^5$ ph/s at the detector faceplate if we put a 10 Å filter in front of it. (The results scale linearly with the filter bandwidth.) The background radiation is about three orders of magnitude lower in a Uranus flyby.

b. N_s is the stray light from the sun. Due to departures from the ideal in any practical telescope, some amount of light that is not admitted in the designed field of view nevertheless reaches the detector. From the specifications of the Large Space Telescope (Ref. 12), this noise is about 10^3 ph $\cdot$ s^{-1} $\cdot$ cm^{-2} $\cdot$ μm^{-1} $\cdot$ sr^{-1} at 0.9 μm, which gives a negligible contribution to the total noise.

c. N_{th} is the thermal noise from the telescope body, roughly given by

$$N_{th} \cong A \cdot 2\pi \cdot \Delta\lambda \cdot 9.1 \cdot 10^{22}\, e^{-\frac{1.54 \cdot 10^4}{T}}, \quad \frac{\text{ph}}{\text{s}} \qquad (2)$$

at $\lambda = 0.9$ μm, where A is the area of the detector in cm^2, $\Delta\lambda$ is the optical bandwidth in Å, and T is the telescope temperature in K. We assume that the detector sees the telescope body through an angle of 2π sr. For T= 300 K, $\Delta\lambda$ = 10 Å, and A = 1 cm^2, we get about 50 ph/s, which is negligible. We note that because of the exponential dependence of N_{th} on the temperature, relatively small changes in T can cause huge changes in N_{th}. For example, if T is increased to 400 K, N_{th} increases to $3 \cdot 10^7$ ph/s, which is no longer negligible.

d. N_1 is the total noise at the output plane of the receiving telescope. The worst case conditions are during flyby encounters, in which case $N_1 \cong N_b$. In other situations, N_{th} can become the dominant component (but this case can be avoided by cooling the detector and restricting the angle at which it sees the telescope body (Fig. 4)).

e. N_γ is the Cherenkov noise due to cosmic-ray activity at the vicinity of the detector (Ref. 13). The basic mechanism is: A high-energy particle enters the photomultiplier faceplate, and photons are emitted and detected by the photocathode. As a rough order of magnitude, the cosmic ray flux above the earth's atmosphere is 1 particle/s-cm^2, and each particle emits about 100 photons. For photomultipliers with 5-cm^2 faceplates this amounts to about 500 ph/s created at the faceplate. Due to geometric considerations and other design procedures, the number actually detected by the photocathode can be reduced by about an order of magnitude. Furthermore, the resulting noise event due to one particle is expected to be a single strong pulse, followed by a few smaller pulses. One could conceivably detect the presence of such an event and partially, if not almost totally, remove its effects.

f. N_d is the noise due to photodetector dark current. Every dark-emitted electron is equivalent to $1/n_p$ noise photons, where n_p is the photodetector quantum efficiency. (In the near infrared, photomultiplier tube (PMT) quantum efficiencies are about 4% at 0.9 μm, 18% at 0.85 μm, and more than 20% at 0.8 μm. Operation around 0.85 μm is probably the most practical due to the availability of laser sources.) The main cause of the dark current at room temperature is thermionic emission, which for typical near-infrared photomultipliers is about 10^4 to 10^5 dark counts per second. This number can be reduced by 3 orders of magnitude by cooling the PMT to about -20°C. An estimate for the photocathode dark current per unit area can be obtained from the Richardson's equation (Ref. 14):

$$I_d = 120\, T^2\, e^{-\frac{E_w}{kT}}, \quad \frac{A}{\text{cm}^2} \qquad (3)$$

where E_w is the photocathode work function (1.38 eV for GaAs). Due to the exponential dependence on the temperature, thermionic emission is negligible once the PMT has been sufficiently cooled.

Other causes of dark current are ohmic leakage, secondary electrons released by ionic bombardment of the photocathode, cold emission from the electrodes, and light feedback to the photocathode. These contributions can be neglected in most practical cases.

g. N_o is the total number of noise photons at the output of the detector obtained by summing the contributions of each noise source. It is important to note that by using a photodetector with high internal gain, one can design the system so that white thermal noise (of the form 4KTB) is not an important noise factor.

IV. Conclusions

In the preceding sections we have surveyed the various noise mechanisms that exist in the link. From the system's operation point of view there are two very different situations. The first occurs during flyby, where the number of noise photons is of the order of 10^5 ph/s (Jupiter and Saturn flyby). The second is not during encounters, where the limiting factor is noise due to other mechanisms, for example, Cherenkov radiation. An intermediate situation is flyby near the outer planets (Uranus and beyond).

References

1. Katz, J., and Lesh, J., *Optical Communication for Deep Space Missions Using Integrated Semiconductor Injection Laser*, JPL Publication. Jet Propulsion Laboratory, Pasadena, Calif., (in preparation).
2. See, for example, Hodara, H., "Laser Wave Propagation Through the Atmosphere," *Proc. IEEE*, Vol. 54, pp. 368-375, 1966.
3. Daniels, G. M., A Night Sky Model for Satellite Search Systems, *Opt. Eng.*, Vol. 16, pp. 66-71, 1977.
4. Roser, S., and Stande, H. J., "The Zodiacal Light from 1500 Å to Micron," *Astron. Astrophys.*, Vol. 67, pp. 381-394, 1978.
5. Leinert, C., "Zodiacal Light – A Measure of the Interplanetary Dust," *Space Sci. Rev.*, Vol. 18, pp. 281-339, 1975.
6. Roach, F. E., and Megill, L. R., "Integrated Starlight over the Sky," *Astrophys. J.*, Vol. 133, pp. 228-242, 1961.
7. Mattila, K., *Synthetic Spectrum of the Integrated Starlight*, Observatory and Astrophysics Laboratory, Tähtitornin mäki, SF-00130, Helsinki, Finland (unpublished).
8. *RCA Electro-Optics Handbook*, chapter 6. Radio Corporation of America, Solid-State Division/Electro-Optics and Devices, Lancaster, Pa., 1974.
9. Harwit, M., *Infrared Astronomical Background Radiation, Infrared Astronomy*, G. Setti and G. G. Facio, editors; pp. 173-180. P. Reidel, Holland, 1978.
10. *The Planets Uranus, Neptune, and Pluto*, NASA SP-8103. National Aeronautics and Space Administration, Washington, D.C., 1971.
11. *The Space Telescope*, NASA SP-392. National Aeronautics and Space Administration, Washington, D.C.
12. *The Space Telescope, Level II*, Interface Requirement Document #STR-02A, July 20, 1978.
13. Young, A. T., "Cosmic Ray Induced Dark Current in Photomultipliers," *Rev. Sci. Inst.*, Vol. 37, pp. 1472-1481, Nov. 1966.
14. See, for example, Angelo, E. J., Jr., *Electronic Circuits*, pp. 60-61, McGraw Hill, New York, 1958.

Table 1. Data for calculating flyby noise from the outer planets

Planet	Approximate distance from the sun $R_{p\odot}$, AU	Radius R, km	Linear FOV from earth, μrad	Geometric albedo at 0.9 μm P_λ	Approximate photon flux E_λ at 0.9 μm, ph / s-cm^2-μm	Approximate number of noise photons/s (LST receiver, 10-A optical filter, 2-μrad detector field of view)
Jupiter	5	71,000	200	0.33	$5 \cdot 10^7$	$2 \cdot 10^5$
Saturn	10	60,000	90	0.33	$4 \cdot 10^{6a}$	$9 \cdot 10^4$
Uranus	20	26,000	17	0.05 ±0.05	$4 \cdot 10^3$	$4 \cdot 10^2$
Neptune	30	25,000	11	0.05 ±0.05	$8 \cdot 10^2$	$9 \cdot 10^1$
Pluto	40	3,000	1	0.15 ±0.1	$1 \cdot 10^1$	$5 \cdot 10^1$

[a]This is an average value; the exact contribution due to the rings must be calculated separately for each case.

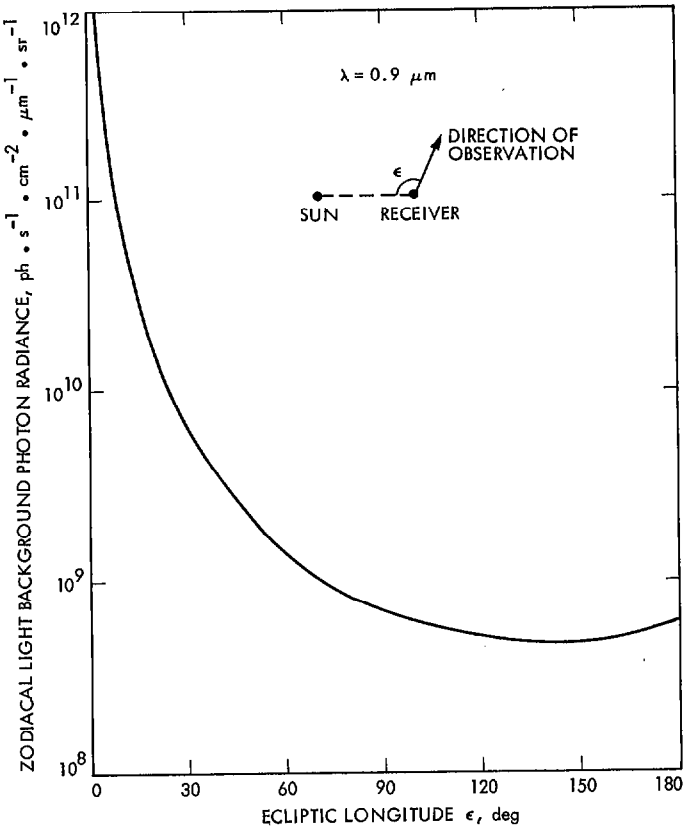

Fig. 1. Zodiacal light photon radiance in the ecliptic plane

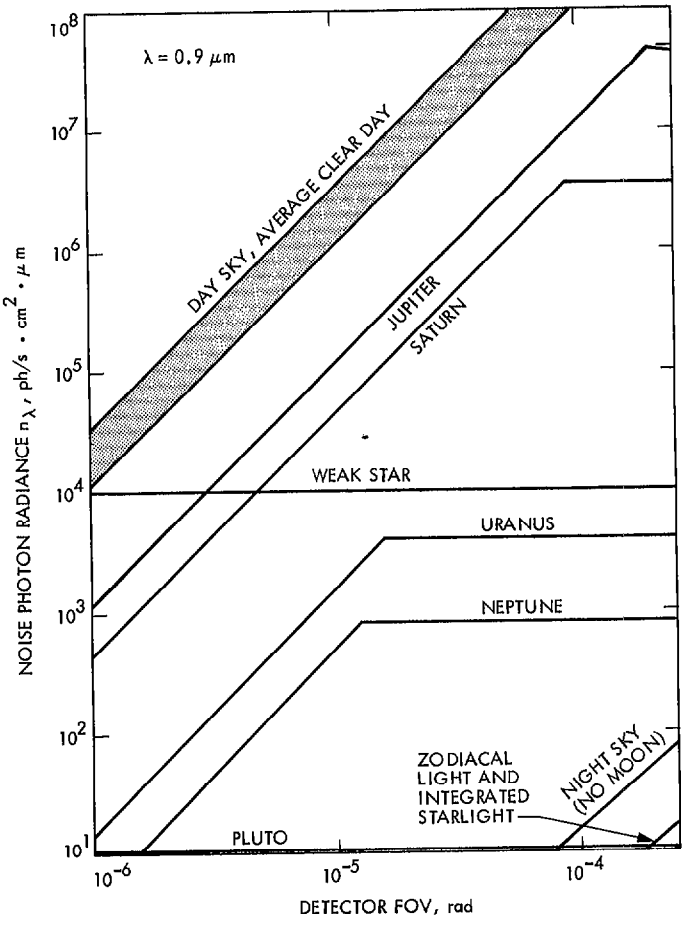

Fig. 2. Background noise radiance vs optical detector field of view

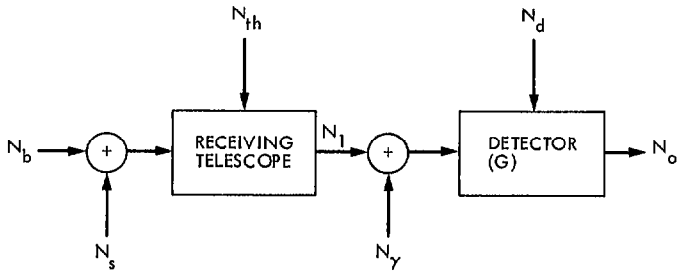

N_b BACKGROUND RADIATION

N_s STRAY LIGHT FROM THE SUN

N_{th} THERMAL RADIATION OF THE TELESCOPE BODY

N_1 TOTAL NOISE OF THE OUTPUT PLANE OF THE RECEIVING TELESCOPE

N_γ CLERNKOV NOISE DUE TO COSMIC RAYS

N_d PHOTODETECTOR DARK CURRENT (DUE TO THERMIONIC EMISSION AND OTHER EFFECTS)

N_o TOTAL NOISE AT THE RECEIVER OUTPUT

NOTE: SINCE A PHOTODETECTOR WITH HIGH GAIN IS USED, THERMAL NOISE IS NEGLIGIBLE

ALL PARAMETERS IN PHOTONS PER SECOND

Fig. 3. Block diagram of noise mechanisms in the optical link

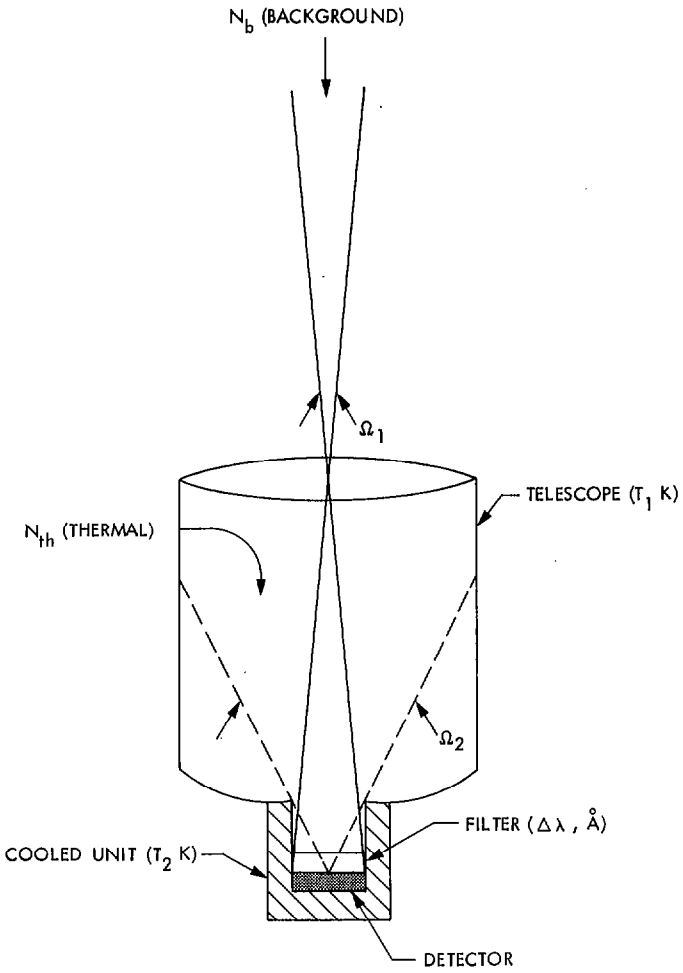

Fig 4. Schematic configuration for noise calculations. The detector "sees" the background noise coming from the angle Ω_1, and the noise due to the telescope thermal radiation coming from the angle Ω_2. With a proper design, one can obtain $\Omega_2 << 2$sr.